Proceedings of the 17th World Congress
The International Federation of Automatic Control
Seoul, Korea, July 6-11, 2008

Robust PID Controller Design for a micro-Actuator with Squeezed Gas Film Damping Effects ⋆

Marialena Vagia * **Anthony Tzes** *

* *Electrical and Computer Engineering Department, University of Patras, Rio, Achaia-26500, Greece.(e-mail:{mvagia,tzes}@ece.upatras.gr).*

Abstract: In this article the modeling aspects of an electrostatic microactuator (μ-A) with squeezed thin film damping effects are presented. The μ-A is composed of a microcapacitor whose one plate is clamped on the ground while the other plate is floating on the air. Its highly nonlinear dynamic model is linearized at various operating points. A robust PID-controller is designed with its parameters-tuning relying on LMIs. This control effort of the PID-controller in collaboration with a feedforward term and a notch filter is applied to the system. Simulation results are used to investigate the efficacy of the suggested control architecture.

1. INTRODUCTION

Planar microstructures fabricated out of metal or heavily doped semiconductors, in relative normal motion have been widely used in the microelectronical devices, such as for positioning (Chen and Dutton (1989); Menciassi et al. (2004); Shao et al. (2004)), flow control problems (Chang (2006)), micromixers and micropumps (Agarwal et al. (2005)), microfabricated propulsion systems (Ketsdeveret al. (2002)), automotive applications using microsensors and micromechatronic actuators (Muller et al. (2003)), RF- MEMS structures (Chia et al. (2007); Rottenberg et al. (2007)).

Electrostatic actuation of microelectromechanical systems (MEMS) (Judy (2001); Rocha et al. (2006); Zhang et all (2003)) utilizes the attractive Coulomb forces that are developed between capacitively coupled semiconductors differing in voltage (Lee et al. (2003)). Their principle of operation is based on the generation of electrostatic forces that are proportional to the square of the applied voltage.

Silicon microstructures (sensors and actuators) that make use of the capacitive measurement principles or electrostatic driving forces, are characterized by very small gaps between the moving surfaces. Subsequently, if one surface moves against the other, the gas in between behaves as a squeezed gas film (Blench (1983); Veijola (2004); Westby and Fjeldy (2002); Vemuri et al. (2000); Veijola et al. (1995)).

In the presence of a compressible gas film, the moving surfaces are forced to squeeze the gas from between them in order to be able to move. Squeeze film effect due to the gas between the moving and stable components strongly affects their performance, and the design and control techniques ought to adapt to this phenomenon. The understanding of the squeeze film damping mechanism in these microactuator (μ-A) devices is necessary in order to optimize the controller designs (Yan and Lal (2006)).

The inclusion of the squeeze film damping effects increases the complexity of the dynamics and appropriate controllers should deal with this fact. Accordingly, as models that describe these systems are highly non-linear and have a large order, the tendency is to design controllers with increased complexity which are difficult to be implemented at the microscopic level. Low-order controllers (on/off, P, PID) are considered the proper match for these μ-As, due to their ease of design and implementation. Rather than relying on a demanding adaptive scheme, accounting for the "augmented dynamics" of the μ-A, simpler control schemes are designed for systems that are good approximations of the "real" plant (Vagia et al. (2006); Lu and Fedder (2004); Sung et al. (2000); Seeger and Boser (2003); Maithripala et al. (2003)). These controllers are easily "implementable" using analog electronic components and thus can be embedded in the μ-A system.

As a minimum requirement, these low complexity controllers, should stabilize the "approximated μ-A system" at any operating point. Moreover, it is desired that the closed loop system be stable for any variations of its linearized system dynamics within the convex-hull of these operating points.

In this article, a "lower order" PID controller (Vagia et al. (2006)) in conjunction with a feedforward term is used at a microactuator. The purpose of the feedforward term is to provide the necessary control input to move the μ-A at a desired operating point. The PID controller's parameters are tuned in order to minimize a certain quadratic cost function. To account for the "operating point" uncertainty, the cost function is minimized over a set of convex constraints and the overall design is cast in a Linear-Matrix Inequalities (LMIs) framework. This LMI-tuned robust PID controller is applied to the augmented system while ensuring its stability. In this article an LMI-

⋆ This paper was partially supported by University of Patras' K. Karatheodoris research initiative program no. C.152

based robust PID controller is designed and applied for controlling the positioning of a μ–A's plate.

In the rest of this article, the model of the μ-A is described in Section 2, while the control architecture of the robust PID controller is presented in Section 3. In Section 4 the simulation results are presented from where the conclusions are drawn in Section 5.

2. MICRO-ACTUATOR MODELLING

The μ-A from a structural point of view corresponds to a micro–capacitor whose one plate is attached to the ground while its other moving plate is floating in the air (Hong et al. (1998); Zarubinskaya and Horssen (2003); Maithripala et al. (2003)). Figure 1 presents the structure of the μ-A. The dynamic nonlinear equation of the system (Tzes et al. (2005); Vagia et al. (2006)) is:

$$m\ddot{\eta} + F_d + k\eta = \frac{\varepsilon A U^2}{2(\eta^{\max} - \eta)^2} = F_{el} \tag{1}$$

where η is the displacement of the plates from the relaxed position, m is the plate's mass, k is the spring's stiffness, A is the area of the plates, U is the applied voltage between the capacitor's plates, $\eta^{\max}$ is the distance of the plates when the spring is relaxed, F_d is the force caused by the parallel plate damper and F_{el} is the electrically-induced force as shown in Figure 2.

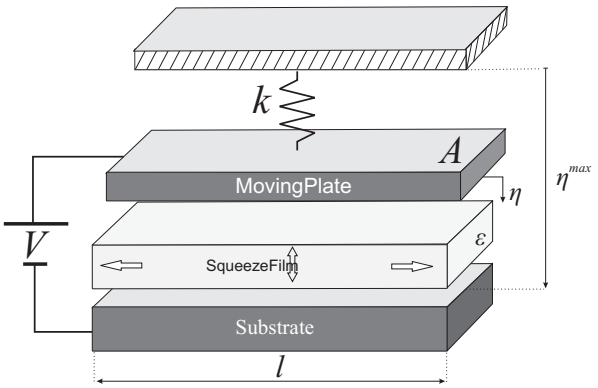

Fig. 1. μ-Actuator structure

2.1 Force caused from the parallel plate damper

Consider the squeezed-film problem, where two surfaces are moving towards each other. When assuming a constant pressure across the gap and when the gap is much smaller than the surface dimensions, the 3–D Navier-Stokes equations are reduced to (Veijola (2004)):

$$\rho\frac{\vartheta u}{\vartheta t} = -\frac{\vartheta p}{\vartheta x} + mi\frac{\vartheta^2 u}{\vartheta z^2} \tag{2}$$

$$\rho\frac{\vartheta v}{\vartheta t} = -\frac{\vartheta p}{\vartheta y} + mi\frac{\vartheta^2 v}{\vartheta z^2} \tag{3}$$

where u and v are the flow velocities in the x, y directions, respectively, mi is the viscosity coefficient, ρ is the density, and p is the pressure of the gas.

Analytic solution for these equations together with their boundaries conditions, can be found, resulting in velocities $u(z,t)$ and $v(z,t)$. The average velocities $\tilde{u}$ and $\tilde{v}$ can be written as

$$\tilde{u} = -\frac{(\eta^{\max} - \eta_i)^2}{12mi} Q_{pr}\frac{\vartheta p}{\vartheta x} \tag{4}$$

$$\tilde{v} = -\frac{(\eta^{\max} - \eta)^2}{12mi} Q_{pr}\frac{\vartheta p}{\vartheta y} \tag{5}$$

where Q_{pr} is the the relative flow rate coefficient that is time dependent due to gas-inertia.

The relative modified Reynolds equation with inertial effects is described as follows:

$$\frac{\vartheta}{\vartheta x}\left(\frac{\rho(\eta^{\max} - \eta)^3}{12mi} Q_{pr}\frac{\vartheta p}{\vartheta x}\right) + \frac{\vartheta}{\vartheta y}\left(\frac{\rho(\eta^{\max} - \eta)^3}{12mi} Q_{pr}\frac{\vartheta p}{\vartheta y}\right) = \frac{\vartheta(\rho(\eta^{\max} - \eta))}{\vartheta t} \tag{6}$$

where Q_{pr} can be approximated by a series expansion as:

$$Q_{pr,\Xi} = \sum_{\xi=1,3,\ldots}^{\Xi} \frac{1}{\frac{\xi^4\pi^4}{96} + \jmath\omega\frac{\xi^2\pi^2\rho(\eta^{\max}-\eta)^2}{96\ mi}} \tag{7}$$

where ξ is an odd integer $\xi \in \{1, 3, \ldots, \Xi\}$.

Solutions for Reynolds equations for rectangular, moving surfaces have been presented by (Veijola (2004); Vemuri et al. (2000); Veijola et al. (1995); Blench (1983)). The structure and dimensions of the damper are presented in Figure (2).

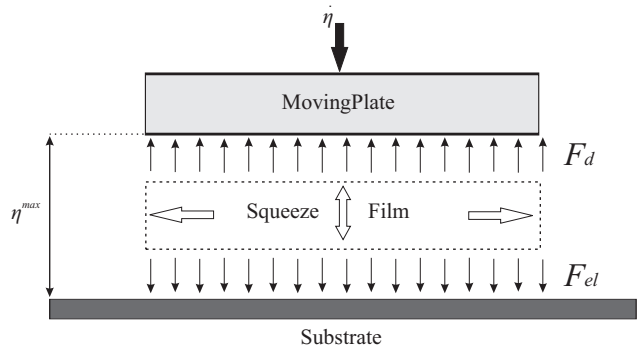

Fig. 2. Diagram of forces applied on the μ-A

The F_d–force acting on the surfaces due to the squeezed film damping effect is:

$$F_d = \sum_{\lambda=1,3,\ldots}^{\Lambda}\sum_{n=1,3,\ldots}^{N} \frac{\dot{\eta}}{Q_{pr,\Xi}G_{\lambda n} + \jmath\omega C_{\lambda n}} \tag{8}$$

with

$$G_{\lambda n} = \frac{\pi^6(\eta_{\max} - \eta)^3(\lambda n)^2}{768 mi l^2}\left(\frac{\lambda^2}{l^2} + \frac{n^2}{l^2}\right) \tag{9}$$

$$C_{\lambda n} = \frac{\pi^4(\eta_{\max} - \eta)(\lambda n)^2}{64 l^2 P_A} \tag{10}$$

where λ and n are odd indices 1,3,5 ..., P_A is the ambient pressure and l is the length of the square plate. After inserting the expression of Q from Equation (7) into Equation (8) the force mapping in the frequency domain is:

$$F_d = \sum_{\lambda=1,3,\ldots}^{\Lambda} \sum_{n=1,3,\ldots}^{N} \frac{\dot{\eta}}{\sum_{\xi=1,3,\ldots}^{\Xi} \frac{1}{R_{\lambda n\xi}+\jmath\omega L_{\lambda n\xi}} + \jmath\omega C_{\lambda n}} \quad (11)$$

where

$$R_{\lambda n\xi} = \frac{\xi^2\pi^4}{96G_{\lambda n}}, \quad L_{\lambda n\xi} = \frac{\xi^2\pi^2\rho(\eta^{\max}-\eta)^2}{96miG_{\lambda n}} \quad (12)$$

where $C_{\lambda n}$ is a reflection of the gas compressibility, and $L_{\lambda n\xi}$ reflects the inertia of the gas. For the given square microcapacitor, the expressions of the aforementioned terms are

$$R_{\lambda n\xi} = \frac{q_1}{(\eta^{\max}-\eta)^3}, \; C_{\lambda n} = q_2(\eta^{\max}-\eta_i), \quad (13)$$

$$L_{\lambda n\xi} = \frac{u_1}{\eta^{\max}-\eta}, \quad (14)$$

where

$$q_1 = \frac{8\ mi\ l^2\xi^4}{\left(\frac{\lambda^2}{l^2}+\frac{n^2}{l^2}\right)\pi^2(\lambda n)^2}, \; q_2 = \frac{\pi^4(\lambda n)^2}{64l^2P_A} \quad (15)$$

$$u_1 = \frac{8\xi^2\rho l^2}{\pi^4(\lambda n)^2\left(\frac{\lambda^2}{l^2}+\frac{n^2}{l^2}\right)} \; . \quad (16)$$

Truncation of the modes utilized in Equation (8) and maintaining the primary one reflected by $\Lambda = N = \Xi = 1$, results in the squeezed film damping description, as:

$$F_d = \dot{\eta}\frac{s\frac{1}{(\eta^{\max}-\eta)q_2} + \frac{q_1}{(\eta^{\max}-\eta)^3u_1q_2}}{s^2 + s\frac{q_1}{(\eta^{\max}-\eta)^2u_1} + \frac{1}{u_1q_2}}. \quad (17)$$

2.2 Linearized Equations of Motion

The nonlinear equation of motion (1) should be linearized at certain operating points in order to design the controller. The "equilibria"-points $\eta_i^o, \; i = 1,\ldots,M$ depend on the applied nominal voltage U_o. Equation (1) for $\dot{\eta}_i^o = 0$ yields

$$k\eta_i^o = \frac{\varepsilon AU_o^2}{2(\eta^{max}-\eta_i^o)^2} \quad U_o = \pm\left[\frac{2k\eta_i^o\left(\eta^{\max}-\eta_i^o\right)^2}{\varepsilon A}\right]^{1/2} \quad (18)$$

This nominal U_o–voltage must be applied if the capacitor's plate is to be maintained at a distance $\eta_i^o \leq \frac{\eta^{\max}}{3}$ from its un–stretched position (Zolotas et al. (2007)) and equals to the feedforward term. This fact must be taken into account as in the presented system a bifurcation point exists at $\eta_i^o = \frac{\eta^{\max}}{3}$. The resulting linearized systems that exist below this point are stable, while the linearized sub–systems above this limit are unstable. In the sequel U_o will be indicated as the "bifurcation parameter" (Khalil (2000)).

The linearized equations of motion around the equilibria points (U_o *and* $\eta_i^o, \dot{\eta}_i^o = 0$) can be found using standard perturbation theory for the variables U and η_i where $U = U_o + \delta u$ and $\eta_i = \eta_i^o + \delta\eta_i$. The linearized equation of motion for the system in (1) is:

$$m\delta\ddot{\eta}_i + F_d^{lin} + k\eta_i^o + k\delta\eta_i = \frac{\varepsilon AU_o^2}{2(\eta^{\max}-\eta_i^o)^2}$$

$$+ \frac{\varepsilon AU_o^2}{(\eta^{\max}-\eta_i^o)^3}\delta\eta_i + \frac{\varepsilon AU_o}{(\eta^{\max}-\eta_i^o)^2}\delta u \; , \quad (19)$$

with $$F_d^{lin} = \delta\dot{\eta}_i\frac{s\overbrace{\frac{1}{(\eta^{\max}-\eta_i^o)q_2}}^{b_{1,i}} + \overbrace{\frac{q_1}{(\eta^{\max}-\eta_i^o)^3u_1q_2}}^{b_{2,i}}}{s^2 + s\underbrace{\frac{q_1}{(\eta^{\max}-\eta_i^o)^2u_1}}_{a_{1,i}} + \underbrace{\frac{1}{q_1q_2}}_{a_{2,i}}}$$

Inserting (18) into (19) when $K_i = \left[k - \frac{\varepsilon AU_o^2}{(\eta^{\max}-\eta_{1,i}^o)^3}\right]$, and $\beta_i = \left[\frac{\varepsilon AU_o}{(\eta^{\max}-\eta_{1,i}^o)^2}\right]$ the state space description of the linearized model is:

$$\begin{bmatrix}\delta\dot{\eta}_i\\ \delta\ddot{\eta}_i\\ \dot{p}_i\\ \ddot{p}_i\end{bmatrix} = \begin{bmatrix}0 & 1 & 0 & 0\\ \frac{-K_i}{m} & 0 & -b_{2,i} & -b_{1,i}\\ 0 & 0 & 0 & 1\\ 0 & 1 & -a_{2,i} & -a_{1,i}\end{bmatrix}\begin{bmatrix}\dot{\eta}_i\\ \ddot{\eta}_i\\ p_i\\ \dot{p}_i\end{bmatrix} + \begin{bmatrix}0\\ \beta_i\\ 0\\ 0\end{bmatrix}\delta u \quad (20)$$

$$= \tilde{A}_i\begin{bmatrix}\dot{\eta}_i\\ \ddot{\eta}_i\\ p_{1,i}\\ p_{2,i}\end{bmatrix} + B_i\delta u \quad i = 1,\ldots,M \quad (21)$$

It should be noted that the elements of the $\tilde{A}_i$ matrix and B_i vector depend on the selected operating point.

In comparison with the classical descriptions, where $F_d^{lin} = b_{dc}\delta\eta_i$, the dc–gain of the transfer function in Equation (17) can be substituted. The dc–gain of the reduced order model is $b_{dc} = \frac{q_1}{(\eta^{\max}-\eta_i^o)^3}$, and the model from (21) can be further reduced to

$$\begin{bmatrix}\delta\dot{\eta}_{1,i}\\ \delta\ddot{\eta}_{1,i}\end{bmatrix} = \begin{bmatrix}0 & 1\\ -\frac{K_i}{m} & -\frac{b_{dc}}{m}\end{bmatrix}\begin{bmatrix}\delta\eta_{1,i}\\ \delta\dot{\eta}_{1,i}\end{bmatrix} + \begin{bmatrix}0\\ \frac{\beta_i}{m}\end{bmatrix}\delta u. \quad (22)$$

$$= \hat{A}_i\begin{bmatrix}\delta\eta_{1,i}\\ \delta\dot{\eta}_{1,i}\end{bmatrix} + B_i\delta u, \quad i = 1,\ldots,M. \quad (23)$$

The "closeness" of this model w.r.t. the one defined in (21) can be traced by their underlying frequency responses. It should be noted that the frequency response of the augmented system description defined in (21) exhibits a lightly damped response at a frequency ω_1; this value depends on the b_i and a_i $, i = 1,2$ parameters. For a better match of these models a notch filter centered at this frequency can be used. The typical transfer function of this filter is

$$F_n = \frac{s^2 + 2s\zeta_1\omega_1 + \omega_1^2}{s^2 + 2s\zeta_2\omega_1 + \omega_1^2}, \; 0 < \zeta_i \leq 1 \; . \quad (24)$$

Its purpose is to allow all frequency content to pass through except the harmonics close to the ω_1–frequency.

The final state space equations for the reduced order system are

$$\begin{bmatrix}\delta\dot{\eta}_{1,i}\\ \delta\ddot{\eta}_{1,i}\end{bmatrix} = \begin{bmatrix}0 & 1\\ -\frac{K_i}{m} & -\frac{b_{dc}}{m}\end{bmatrix}\begin{bmatrix}\delta\eta_{1,i}\\ \delta\dot{\eta}_{1,i}\end{bmatrix} + \begin{bmatrix}0\\ \frac{\beta_i}{m}\end{bmatrix}\delta u. \quad (25)$$

$$= \hat{A}_i\begin{bmatrix}\delta\eta_{1,i}\\ \delta\dot{\eta}_{1,i}\end{bmatrix} + B_i\delta u, \quad i = 1,\ldots,M. \quad (26)$$

If a controller design is to rely on these reduced order dynamic model, the control effort should be filtered through the aforementioned notch filter.

3. ROBUST PID CONTROLLER DESIGN

The feedback term is a robust PID controller for the set of the M–linearized systems in (26). The LMI–based (Ge et al. (2002)) PID controller design procedure is based on the theory of Linear Quadratic Regulator (LQR).

This robust PID controller is specially designed to address the case where multiple–models (Cheng and Yu (2000); Hongfei and Jun (2001)) have been utilized in order to describe the uncertainties that are inherent from the linearization process of the non–linear system model. The architecture of the control scheme is presented in Figure 3.

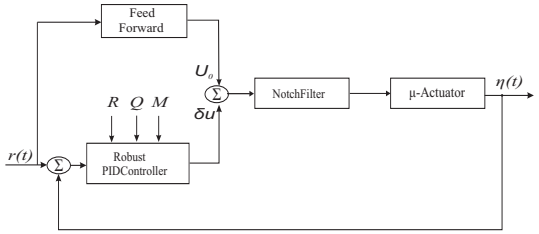

Fig. 3. Controller Architecture

The nature of a PID–structure in the controller design can be achieved if the linearized system's state vector $\bar{\eta} = [\delta\eta_i, \delta\dot{\eta}_i]^T$ is augmented with the integral of the error signal $\int edt = \int (r(t) - \eta_i(t))\, dt$. In this case, the augmented system's description is:

$$\begin{bmatrix} \dot{\bar{\eta}}_i \\ -e \end{bmatrix} = A_i \begin{bmatrix} \bar{\eta}_i \\ -\int edt \end{bmatrix} + \begin{bmatrix} B_i \\ 0 \end{bmatrix} \delta u + \begin{bmatrix} -1 \\ 0 \end{bmatrix} r, \qquad (27)$$

where $A_i = \begin{bmatrix} \hat{A}_i & 0 \\ 1 & 0 \end{bmatrix}$.

The LQR–problem for the systems described in (27) can be cast in the computation of δu in order to minimize the cost:

$$J(\delta u) = \int_0^\infty (\tilde{\eta}^T\ Q\ \tilde{\eta} + \delta u^T\ R\ \delta u) dt \qquad (28)$$

where $\tilde{\eta} = \left[\bar{\eta}, -\int edt\right]^T$, and Q, R are semidefinite and definite matrices respectively. The solution to the LQR problem relies on computing a common Lyapunov matrix that satisfies the Algebraic Ricatti Equations (AREs):

$$A_i^T P + P A_i - P B_i R^{-1} B_i{}^T P + Q = 0,\ i = 1, \ldots, M \qquad (29)$$

It should be noted that the optimal cost at (28) is equal to $\tilde{\eta}^T(0)\hat{P}^{-1}\tilde{\eta}(0)$ for a P-matrix satisfying (29). An efficient alternative for the optimal control $\delta u = -S\tilde{\eta}$ can be computed by transforming the aforementioned optimization problem subject to the concurrent satisfaction of the AREs (29) into an equivalent LMI–based algorithm (Boyd et al. (1994)), where a set of auxiliary matrices $\hat{P}$, Y and an additional variable γ ($\gamma > 0$) have been introduced.

$$\min \gamma$$

$$\text{subject to} \begin{cases} \begin{bmatrix} \gamma & \tilde{\eta}^T(0) \\ \tilde{\eta}(0) & \hat{P} \end{bmatrix} \leq 0 \\ \begin{bmatrix} A_i\hat{P} + \hat{P}A_i^T + B_iY + Y^TB_i^T & \hat{P} & Y^T \\ \hat{P} & -Q^{-1} & 0 \\ Y & 0 & -R^{-1} \end{bmatrix} \leq 0 \\ \text{for } i = 1, \ldots, M \\ \hat{P} > 0 \end{cases}$$

The feedback control can be computed based on the recorded values of $\hat{P}^*$ and Y^* for the last feasible solution:

$$\delta u = Y^*(\hat{P}^*)^{-1}\tilde{\eta} = -S\tilde{\eta} = -S \begin{bmatrix} \bar{\eta} \\ -\int edt \end{bmatrix} \qquad (30)$$

$$= -\left[\, s_p \,|\, s_d \,|\, s_i \,\right] \begin{bmatrix} \delta\eta_i \\ \delta\dot{\eta}_i \\ -\int edt \end{bmatrix}$$

$$= \left[s_p e + s_d \dot{e} + s_i \int edt \right] + \left[s_p \left(\eta_i^o - r\right) - s_d \dot{r} \right]. \qquad (31)$$

The first portion of the controller form in (31) is equivalent to that of a PID–controller.

This controller is applied and tested on the augmented order system and simulation studies prove the efficacy of the suggested scheme.

3.1 Closed-Loop Switching-System Behavior

When the μ-A's plate moves at different operating points η_i^o during its travel there are switchings in the linearized subsystems. Since there is no guarantee that the advocated suboptimal controller can tolerate these switchings, an a posteriori technique is used to determine (at a minimum) the stability of the switched closed-loop system (Gahinet et al. (1996); Hongfei and Jun (2001)).

The used theory relies on the notation of quadratic stability, where the closed-loop system:

$$\dot{w} = A_{cl}^i w \qquad (32)$$

where A_{cl} denotes the closed-loop system's matrix, the state vector w contains the states of the system $[\delta\eta, \delta\dot{\eta}]$ and those of the controller. Since the plant's nominal matrices $A_i \in \{A_1, \ldots, A_M\}$, then the closed-loop switches on the vertices $A_{cl}^i \in \{A_{cl}^1, \ldots, A_{cl}^M\}$. The stability of the switching closed-loop system is guaranteed if a symmetric positive matrix Q can be found such that:

$$A_{cl}^i Q + Q A_{cl}^{iT} + A_{cl}^j Q + Q A_{cl}^{jT} < 0 \qquad (33)$$

$$\forall i, j \in \{1, \ldots, M\}$$

$$Q > 0 \qquad (34)$$

It should be noted that the a posteriori nature of the investigation of the system's stability is due to the computation of Q from the LMIs (33, 34) after the formulation of the feedback controller.

4. SIMULATION RESULTS

Simulation studies were carried on a μ-A's non–linear model, whose plates are made of SiO_2.The parameters of the system are presented in the following Table:

parameter	Description	Value	Unit
A	Area of the plates	$1.6\ 10^{-7}$	m
η^{max}	Distance between the plates	$4\ \times 10^{-6}$	m
l	Length	$400\ \times 10^{-6}$	m
mi	Viscosity Coefficient	$18.5\ \times 10^{-6}$	kgm/sec^2
ρ	Density	1.155	kg/m^3
ε	Dielectric constant of the air	$8.85\ \times 10^{-12}$	$coul^2/Nm^2$
P_a	Ambient Pressure	10^5	N/m^2
k	Stiffness of the spring	0.816	N/m

The allowable displacements of the micro–capacitor's plate in the vertical axis were $\eta \in [0.1, 1.3]\,\mu$m=$[\eta_o^{\min}, \eta_M^{\max}]$. This is deemed necessary in order to guarantee the stability of the linearized open–loop system.

Figure 4 shows the relationship between the squeezed gas film damping dc–gain coefficient of the linearized open loop "augmented" system, and the distance between the plates of the μ-A. It should be noted that at the "bifurcation" point the dc–gain switches its sign and results in an unstable open loop system.

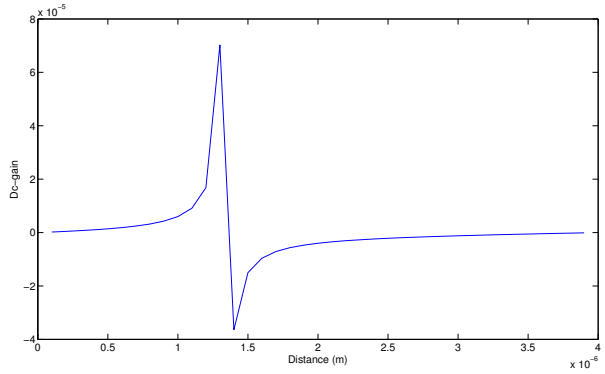

Fig. 4. Squeezed gas film damping b_{dc}–coefficient w.r.t. mu–A plate gap

The Bode diagrams of the "augmented" system, the reduced order system and the augmented system in cascade with the notch filter are presented in Figure 5. It is apparent that the notch filter reduces the peak of the underdamped augmented system by apprxoimately 50 dB.

The goal of the controller is to move the capacitor's plates from an initial position to a new desired one (set–point regulation), and simulation studies were carried on the non–linear model of the μ-A system.

In the sequel, two cases are examined; in the first one, only 1 linearized point at $\eta_i^o = 0.7\mu$m was used while in the second one 15 points $\eta_i^o = 0.1 + \frac{1.33-0.1}{15}(i-1)\ \mu$m $i = 1, \ldots, 15$ were utilized. The upper plate is allowed to travel in the range of $[0.1, 1.33]\,\mu$m. In the sequel, unless otherwise stated the parameters used in the formulation of the LQR–cost were $R = 10^{-8}$ and $Q = 10^{-6}\mathbf{I}_{3\times 3}$.

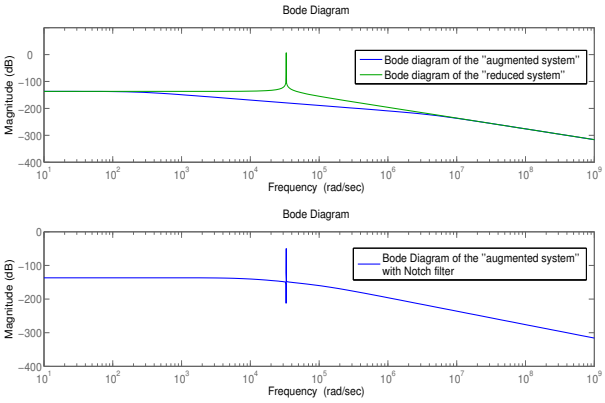

Fig. 5. Bode diagrams of the linearized systems

The proposed control scheme was applied in multiple simulation test cases in order to test its efficacy. For simulation purposes, and while the micro–actuator is at rest at 0.3μm ($\eta_i(0) = 0.9\mu$m), the μ-Actuator's plate is asked to move in a step-fashion to 0.9 μm. In Figure 6, the responses of the μ-A's plate for $M = 1$ and $M = 15$ are presented. Comparing the responses an apparent velocity improvement is observed when using more operating points.

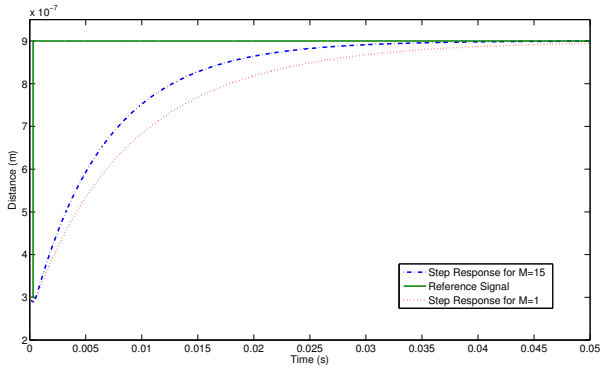

Fig. 6. Step Response of the non-linear controller μ-A system

Finally the frequency content of the PID controller's effort is presented in Figure 7, from where it is shown that it is mainly affecting the lower frequency spectrum.

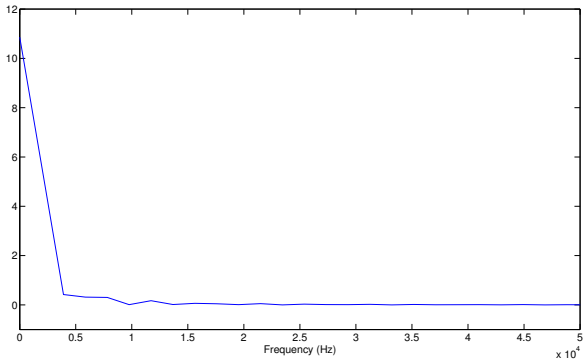

Fig. 7. Frequency content of control effort

5. CONCLUSION

In this article a robust PID controller tuned with the theory of LMIs has been designed for an approximated model of a μ-A with squeeze film gas film damping effect. The control effort is filtered through a notch filter for eliminating the harmonics around a frequency dictated by the system's characteristics. The robust control scheme has been applied on the μ-A's non–linear system in order to prove its efficacy.

REFERENCES

A. Agarwal, S. Sridharamurthy, D. Beebe, 2005. Programmable autonomous micromixers and micropumps.

IEEE Journal of Microelectromechanical Systems 14. pp. 1409-1421.

J.J. Blench, 1983. On isothermal Squeeze Films. Journal of Lubrication Technology. 105. pp.615-620.

S. Boyd, L. Ghaoui, E. Feron and V. Balakrishnan, 1994. Linear Matrix Inequalities in System and Control Theory. SIAM Studies in Applied Mathematics, 1994 Philadelphia PA.

S. Chang, 2006. Demonstration of robust micromachined jet technology and its application to realistic flow control problems 20. pp. 554560. Journal of Measurement Science and Technology.

E. Chen and R.W. Dutton, 2000. Electrostatic Micromechanical Actuator with extended range of travel Journal of microelectromechanical Systems 9. pp. 321–328.

Y. Cheng and C. Yu, 2000. Nonlinear process control using multiple models: relay feedback approach Industrial Eng.Chem. 39. pp. 420–431.

C. H. Chu, W. P. Shih, S. Y.Chung, H. C. Tsai, T. K. Shing and P. Z. Chang 2007. A low actuation voltage electrostatic actuator for RF MEMS switch applications J. Micromech. Microeng 17. pp. 1649-1656.

Gahinet P., Apkarian P., Chilali M. 1996. Affine parameter-dependent Lyapunov functions and real parametric uncertainty IEEE Transactions on Automatic Control 41. pp. 436–442.

M. Ge, M. Chiu and Q. Wang, 2002. Robust PID controller Design via LMI approach. Journal of Process Control 12. pp. 3–13.

S. Hong, V. Varadan and V. Varadan, 1998. Implementation of coupled mode optimal structural vibration control using approximated eigenfunctions. Smart Material Structures 7. pp. 63–71.

S. Hongfei and Z. Jun, June 2001. Control Lyapunov functions for switched control systems. In the Proceedings of the 2001 American Control Conference, Virginia, pp. 1890–1891 June 2001.

J. Judy, 2001. Microelectromechanical systems (MEMS): fabrication, design and applications. Smart materials and Structures. 10. pp. 1115–1134.

A. Ketsdever, R. Lee and T. Lilly, 2005. Performance testing of a microfabricated propulsion system for nanosatellite applications. Journal of Micromechanics and Microengineering. 15. pp. 2254–2263.

H. K. Khalil 2000. Performance testing of a microfabricated propulsion system for nanosatellite applications. Journal of Micromechanics and Microengineering. 15. pp. 2254–2263.

A. Lee, C. McConaghy, G. Sommargren, P. Krulevitch and E. Campbell, 2003. Vertical - actuated electrostatic comb drive with in situ capacitive position correction for application in phase shifting diffraction interferometry. Journal of Microelectromechanical Systems 12. pp. 960–971.

M. S. C. Lu and G. Fedder, 2004. Position Control of Parallel-Plate Microactuators for Probe-Based Data Storage. Journal of microelectromechanical Systems 13. pp. 759–769.

E. Lyshevski, 1998a. Microelectromechanical systems: Motion control of microactuators. IEEE/ASME Transactions on Mechatronics 10. pp. 363–385.

D. Maithripala, J. Berg and P. Dayawansa, 2003. Control of an Electrostatic Microelectromechanical System Using Static and Dynamic Output Feedback. ASME's Journal of Dynamic Systems, Measurement, and Control 127. pp. 443–450.

A. Menciassi, A. Eisinberg, I. Izzo and P. Dario, 2004. From "macro" to "micro" Manipulation: Models and Experiments.IEEE-ASME Transactions on Mechatronics 9. pp. 311–320.

R. Muller-Fiedler, V. Knoblauch,2003. Reliability aspects of microsensors and micromechatronic actuators for automotive applications. Journal of Microelectronics Realibility. 43. pp.1085–1097, 2003.

A. Rocha, E. Cretu and R. F. Wolffenbuttel, 2006. Using dynamic voltage drive in a parallel-plate electrostatic actuator for full-gap travel range and positioning. Journal of Microelectromechanical Systems 15. pp. 69–83.

X. Rottenberg, S. Brebels1, P. Ekkels, P. Czarnecki, P. Nolmans, R. P. Mertens, B. Nauwelaers, R. Puers, I. De Wolf, W. De Raedt and H. A. C. Tilmans, 2007. An electrostatic fringing-field actuator (EFFA): application towards a low-complexity thin-film RF-MEMS technology. J. Micromech. Microeng 17. pp. 204-210.

J. I. Seeger and B. E. Boser, 2003. Charge control of parallel-plate, electrostatic actuators and the tip-in instability. Journal of Microelectromechanical Systems 12. pp. 656–671.

Y. Shao, D. L.Dickensheets and P. Himmer, 2004. 3-D MOEMS mirror for laser beam pointing and focus control. IEEE Journal of Selected Topics in Quantum Electronics 10. pp. 528–535.

L. Sung, Q. K. Yongsang and G. Dae-Gab, 2000. Continuous gain scheduling control for a micro-positioning system: Simple, robust and no overshoot responser. Control Engineering Practice 8. pp. 133–138.

A. Tzes, G. Nikolakopoulos, L. Dritsas and Y. Koveos, 2005. Multi–parametric H_∞ control of a μ–actuator. Proceedings of the IFAC World Congress (Prague, Czech) Article no.4455.

M.Vagia, Nikolakopoulos G. and Tzes A., 2006. Intelligent Robust Controller Design for a micro–Actuator. Journal of Intelligent and Robotic Systems 47. pp. 299-315.

T. Veijola 2004. Compact models for squeezed-film dampers with inertial effects. In the proceedings of the Conference of Design, Test, Integration and Packaging of MEMS/MOEMS,DTIP, Montreux, Switcherland May 2004.

T. Veijola, H. Kuisma, J. Lahdenpera and T. Ryhanen 1995. Equivalent-circuit Model of squeezed gas film in a silicon accelerometer. Sensors and Actuators A. 48. pp.239-248.

S. Vemuri, G.Fedder and T. Mukheree 2000. Low-order Squeeze film model for simulation of MEMS devices. 2000 International Conference on Modeling and Simulation of Microsystems. San Diego, USA March 2000. pp.205 - 208

E. Westby and T.A. Fjeldy 2002. Dynamical Equivalent-Circuit Modelling of MEMS with Sqeezed Gas Film Damping. Physical Scripta. 101. pp.192-195.

D. Yan and A. Lal 2006. The squeeze film damping effect of perforated microscanners: modeling and characterization. Smart Materials and Structures. 15. pp.480-484.

M. Zarubinskaya and W. Horssen, 2003. On the free vibrations of a rectangular plate with two opposite sides simply supported and the other sides attached to linear springs. Journal of Sound and Vibration 278. pp. 1081–1093.

H. Zhang, A. Laws, V.Bright, K. Gupta and Y. Lee, 2003. MEMS variable - capacitor phase shifters Part I: Loaded - line phase shifter. International Journal of RF and Microwave Computer - Aided Engineering 13. pp. 321–337.

A. Zolotas,A. Tzes and M. Vagia, 2007. Robust Control Design for an Uncertain Electrostatic Micro-Mechanical System via Loop Shaping. In the Proceedings of the European Control Conference (ECC' 07), Kos, Greece July 2007 pp.389-395.